

# Channel Model for Monte-Carlo Simulation of Data Transmission on Terrestrial FSO Paths

Zdenek Kolka, Viera Biolkova, and Dalibor Biolek

**Abstract**—The paper deals with a fully parameterized model for Monte-Carlo simulation of data transmission on atmospheric Free-Space Optical (FSO) paths. Due to the effect of atmospheric turbulence the channel is characterized by signal fluctuation in the order of tens of milliseconds, which is several orders of magnitude longer than the duration of transmitted packets. For moderate transmission rates the FSO channel can be simply modeled as a channel with slowly varying random attenuation, which is generated by the proposed model by means of low-pass filtering a random number sequence. The probability of occurrence of errors in each packet can be computed using analytical formulae based on the generated signal level. The model has been implemented into the OMNeT++ simulator.

**Keywords**— Atmospheric turbulence, data transmission, free-space optical links, Monte-Carlo simulation, network simulation.

## I. INTRODUCTION

THE technology of point-to-point Free-Space Optical (FSO) links consists in transmitting information by means of narrow light beams in space or in the atmosphere. At present, terrestrial systems of up to gigabit capacity with a range of up to several kilometers are commercially available. The majority of the links are designed as simple protocol-independent repeaters on the physical layer, using on-off keying (OOK) of laser diode or LED in the transmitter. Other types (ground-space, e.g.) are still in experimental stage [1].

The development of terrestrial FSO systems towards higher data rates, better reliability and network performance requires abandoning the simple repeater design. A number of nontrivial communication techniques based on detailed analyses of the atmospheric channel have been proposed (see [2] for a comprehensive review).

The atmosphere causes long outages due to the occurrence of fog, heavy rain and snow, and relatively short outages on the millisecond scale due to atmospheric turbulence. The long outages are the main phenomena influencing short-range links. Statistical data for large territories can be obtained from long-term meteorological observations [3]. The link availability depends on the value of the fade margin. With respect to safety

regulations and available components, carrier-grade availability can be obtained only for very short links ( $\approx 100$  m for the temperate climate) or in combination with a microwave link [4], [5].

Long-range terrestrial links with a tight power budget are, in addition, influenced by atmospheric turbulence. Inhomogeneity in the atmosphere causes power fluctuations at the receiver on the millisecond time scale for static terminals and on the microsecond time scale for airborne terminals. These short outages increase the bit-error rate and interfere with communication protocols.

A general theory of turbulence can be found in the classical book [6]. Theoretical information capacity of the channel was analyzed in [7]. However, a number of studies have shown suboptimal performance of the TCP, the most popular transport-layer protocol, over the turbulent channel. The TCP congestion-avoidance mechanism misinterprets the short fades, which results in decreased data rates (see e.g. [8]). Therefore a number of FEC coding schemes, diversity techniques, or link-layer protocols have been proposed to mitigate the fades [2], [10].

The analysis of the performance of proposed communication techniques is usually based on statistical models, which are powerful tools when it is possible to describe the protocol analytically or in the form of Markov process. Paper [9] analyzes the performance of TCP over the turbulent atmospheric optical channel using a two-state continuous-time Markov process, where the durations of “good” and “outage” states were modeled by exponential distribution. In [8] a 3D Markov model is used to analyze various flavors of TCP, including the exponential back-off.

On the other hand, in cases when a simple solvable model cannot be formulated, the time-domain (Monte-Carlo) simulation can be used for protocols of any complexity at the expense of computational cost. Multivalued Markov models [9], [12] provide discrete power levels, which may not be suitable for short-term BER calculation. Moreover, there is no clear link to the FSO design parameters. Paper [11] proposes a channel model in terms of a pair of stochastic differential equations which can be numerically evolved in time to produce continuous-value time records of faded optical intensities. However, the parameters of the model can only be identified from measured time series. A feasible method for generating scintillations was proposed in [13]. A Gaussian random number generator with a suitable low-pass filter

Zdenek Kolka is with the Department of Radio Electronics, Brno University Technology, Brno, Czech Republic (e-mail: kolka@feec.vutbr.cz).

Viera Biolkova is with the Department of Radio Electronics, Brno University Technology, Brno, Czech Republic (e-mail: biolkova@feec.vutbr.cz).

Dalibor Biolek is with the Department of Microelectronics, Brno University Technology, Brno, Czech Republic (e-mail: biolek@feec.vutbr.cz).

simulates the fluctuating received optical power.

The paper adopts the method from [13] to develop a fully parameterized model simulating packet transmission in IM/DD FSO systems over a turbulent channel. It is based on the assumption that the packet duration is shorter by orders of magnitude than the channel correlation time. Then it is possible to calculate directly the short-time BER and the probability of successful packet transmission even for link implementations using frame-level FEC. The model was implemented in the OMNeT++ network simulator as a custom channel.

Section 2 explains the model and Section 3 presents a comparison between measured and simulated data.

## II. FSO LINK MODEL

### A. Power Budget

Let us consider the point-to-point FSO terrestrial link in Fig. 1.

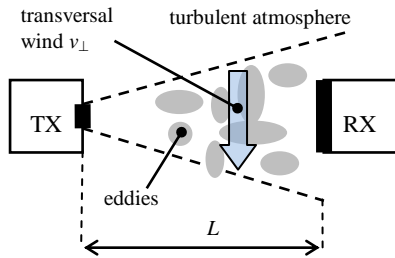


Fig. 1 FSO link configuration

With respect to the expected channel linearity the received optical power  $p_{RX}$  can be expressed as

$$p_{RX} = p_{TX} a_{FSL} a_p a_{ATM} a_T. \quad (1)$$

To avoid unnecessary complexity of the model, both the transmitted  $p_{TX}$  and the received  $p_{RX}$  optical powers are related to the transmitting and receiving apertures, respectively.

Let us assume the diameter of the optical beam at the receiver is large enough for the whole receiving aperture to be uniformly irradiated. Then the free space propagation coefficient  $a_{FSL}$  at the beam center can be simply expressed as

$$a_{FSL} = \left( \frac{D_{RX}}{\theta_{TXe} L} \right)^2, \quad (2)$$

Where  $L$  is the channel distance,  $D_{RX}$  is the receiver aperture diameter, and  $\theta_{TXe}$  is the divergence full angle of the equivalent beam with uniform distribution of irradiance. For an ideal top-hat beam,  $\theta_{TXe}$  represents its divergence full angle. For the Gaussian beam  $\theta_{TXe} = \theta_{Gauss} / \sqrt{2}$ . The possible pointing error is represented by the pointing-loss coefficient  $a_p$ .

Transmission coefficient  $a_{ATM}$  represents the atmospheric attenuation caused by absorption and scattering, which increases significantly during fog, rain, and snowfall, and may cause a long outage. It is a very slow process, which

determines the overall link availability [3], [5].

The term  $a_T$  represents the effect of atmospheric turbulence, which just redistributes energy in the beam with no energy loss. When the receiving aperture is smaller than the beam cross-section, the received power fluctuates.

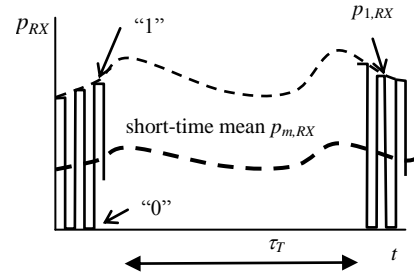


Fig. 2 Received optical power (ON-OFF keying shown)

Equation (1) comprises three processes with very different time scales, which can be described by the relation

$$\tau_{DATA} \ll \tau_T \ll \tau_{ATM}, \quad (3)$$

Where  $\tau_{DATA}$  represents the duration of transmitted packets,  $\tau_T$  is the “period” of atmospheric turbulence, and  $\tau_{ATM}$  represents slow atmospheric processes (fog, snow, etc.). Typical values are  $\tau_{DATA} \approx \mu s$ ,  $\tau_T \approx 1ms - 10ms$ ,  $\tau_s > 1min$ .

Considering the equal probability of the symbols “0” and “1” and with respect to (3) we can define the short-time mean power at the receiver as

$$p_{m,RX} = 0.5 p_{1,RX}, \quad (4)$$

which fluctuates randomly due to atmospheric turbulence.  $p_{1,RX}$  is the received power for the symbol “1”, see Fig. 2.

### B. Packet erasure probability

The inequality (3) greatly simplifies the channel modeling. Considering transmission rates of 100Mb/s and above, an interval of 100 $\mu s$ , during which the received power is practically constant, corresponds to a block of more than  $10^4$  bits. Bit error probability during the interval depends on constant signal-to-noise ratio in the receiver. Thus the optical atmospheric channel can be modeled by a slowly varying “short-time” bit error rate [14].

For On-Off Keying a realistic formula for the short-time BER was proposed in [14]

$$P_b = Q \left[ \frac{p_{m,RX} / P_N}{1 + \sqrt{1 + \xi_0 p_{m,RX} / P_N}} \right], \quad (5)$$

Where the empirically determined parameters  $P_N$  and  $\xi_0$  characterize the equivalent optical noise properties of the whole receiver, and  $Q$  is the standard Gaussian tail integral. The formula was derived for the adaptive decision threshold in the receiver and for the infinite extinction ratio of the transmitter.

A detailed characterization of optical receiver for

calculating (5) may not be always available. In many cases just an optical power level  $p_{m0}$  for a given  $P_{b0}$  is specified (for example, for  $P_{b0} = 10^{-9}$  or  $P_{b0} = 10^{-12}$ ). Considering the shot-noise coefficient in (5)  $\xi = 0$  the noise floor  $P_N$  can be estimated as

$$P_N = \frac{P_{m0}}{-F^{-1}(P_{b0})} = \frac{P_{m0}}{\sqrt{2} \operatorname{erfc}^{-1}(2P_{b0})}, \quad (6)$$

Where  $F^{-1}$  is the normal inverse cumulative distribution function and  $\operatorname{erfc}^{-1}$  is the inverse complementary error function.

In the case of a simple FEC coding on the link layer the transmitted frame of  $n$  bits will be lost (or “erased”) with the probability

$$P_F = 1 - \sum_{i=0}^{N_{FEC}} \binom{n}{i} P_b^i (1 - P_b)^{n-i} \quad (7)$$

Given by the binomial distribution as the bit errors are independent.  $N_{FEC}$  is the acceptable number of errors in the frame. For links without forward error correction,  $N_{FEC} = 0$ .

After calculating (7) the packet is marked as lost during Monte-Carlo simulation in case

$$\chi < P_F, \quad (8)$$

Where  $\chi$  is a random number with uniform distribution on (0, 1).

### C. Atmospheric turbulence

Atmospheric turbulence is represented by randomly varying coefficient  $a_T$  in (1) with unity mean and variance  $\sigma_T^2$ , which characterizes the depth of scintillations and is called the *Power Scintillation Index* (PSI).

From the theory of turbulence it follows that  $a_T$  has the lognormal statistics in the weak turbulence (for  $\sigma_T^2 < 1$ ) and the Gamma-Gamma statistics in the moderate and strong turbulence for point receiver [6]. However, for apertures comparable to the correlation length

$$\rho_C \approx \sqrt{L\lambda} \quad (9)$$

Or larger the irradiance fluctuations are “averaged” and the received power statistics can be approximated by lognormal distribution [15]. The larger the receiver aperture, the more uncorrelated contributions are summed at the photodetector.

Let us consider the lognormal PDF of  $a_T$  in the form

$$f_{a_T}(a) = \frac{1}{a\sigma_L\sqrt{2\pi}} \exp\left(-\frac{[\ln a + \sigma_L^2/2]^2}{2\sigma_L^2}\right), \quad (10)$$

Where  $\sigma_L$  is the log variance related to PSI as

$$\sigma_L^2 = \ln(\sigma_T^2 + 1). \quad (11)$$

The log variance can also be approximated from the channel

parameters [6]

$$\sigma_L^2 = \exp\left[\frac{0.49\sigma_R^2}{(1+0.18d^2+0.56\sigma_R^{12/5})^{7/6}} + \frac{0.51\sigma_R^2}{(1+0.9d^2+0.62d^2\sigma_R^{12/5})^{5/6}}\right] - 1, \quad (12)$$

Where

$$d = \sqrt{k D_{RX}^2 / 4L}, \quad (13)$$

$k = 2\pi / \lambda$  is the wave number. In the case of plane wave propagation the Rytov variance  $\sigma_R^2$  is given as

$$\sigma_R^2 = 1.23 C_n^2 k^{7/6} L^{11/6}, \quad (14)$$

Where  $C_n^2$  is the index of the refractive structure parameter determining the turbulence strength. Typically,  $C_n^2$  varies from  $10^{-17}$  to  $10^{-13}$  according to the strength of atmospheric turbulence.

A method for generating a random  $a_T$  including its spectral properties was suggested in [13], Fig. 3. The zero-mean Gaussian random number generator produces a sequence  $z_i$ , which is filtered in a low-pass FIR filter to obtain a band-limited discrete signal  $x_i$ . The final nonlinear block transforms the normal sequence  $x_i$  to a lognormal  $a_{Ti}$  as specified in (10).

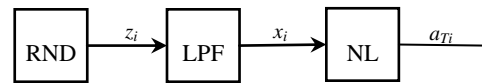


Fig. 3 Generation of samples of random signal  $a_T$

Based on turbulence theory the autocorrelation function of the log amplitude of scintillation can be approximated as [13]

$$R_{\ln a_T}(\tau) = \sigma_L^2 \exp\left[-(\tau/\tau_0)^2\right], \quad (15)$$

Where  $\tau_0$  is the turbulence correlation time. Using the Taylor principle of *frozen turbulence*, the “frequency” of scintillations is proportional to the transversal wind speed. The *eddies* in Fig. 1 can be thought of as carried by the transversal component  $v_{\perp}$  of wind (or by the relative speed of mobile terminal) [6]. The correlation time is then

$$\tau_0 = \rho_C / v_{\perp}. \quad (16)$$

Using the Wiener-Khinchin theorem, the continuous transfer function of LPF in Fig. 3 can be obtained from (15) [13]

$$H(f) = \sqrt{\sigma_L^2 \tau_0} \sqrt{\pi} \exp\left[-\frac{1}{2}(\pi \tau_0 f)^2\right] \exp[-j2\pi f T_d], \quad (17)$$

Where  $T_d$  is an added delay to make the filter causal. Using a standard procedure of FIR filter design, for example from [16], the filter impulse response  $h_k$ ,  $0 \leq k \leq M-1$ , with a

sampling period  $t_s$  can be obtained. The output discrete-time signal  $x_i$  is then

$$x_i = \sum_{k=0}^{M-1} h_k z_{i-k}. \tag{18}$$

Let us suppose the filter is supplied by uncorrelated random numbers  $z_i$  with variance  $\sigma_G^2$  from the RND block, see Fig. 3. After an initial transient of  $M$  samples, each  $x_i$  is given as a sum of  $M$  normal random numbers weighted by  $h_k$ . Therefore the log variance (of  $x_i$ ) will be

$$\sigma_L^2 = \sigma_G^2 \sum_{k=0}^{M-1} h_k^2. \tag{19}$$

Finally, the band-limited normal random sequence  $x_i$  is transformed into  $a_{Ti}$  by

$$a_{Ti} = \exp(x_i - \sigma_L^2/2), \tag{20}$$

Which stems from the well-known relation between normal and lognormal distributions.

*D. Event-driven simulation*

The simulation in OMNeT++ (or other network simulators) is event-driven, i.e. the model procedure is “woken up” at the time of packet transmission while the generating process in Fig. 3 works with equidistant sampling. The implemented solution is shown in Fig. 4.

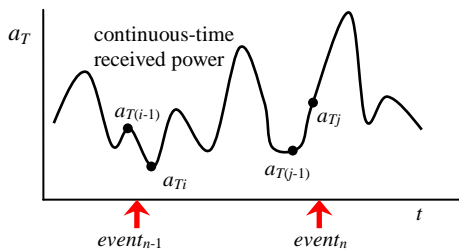


Fig. 4 Generating  $a_{Ti}$  in event-driven environment

The  $M$  random numbers  $z_i$ , which are used to compute the log amplitude (18), are held in a circular buffer. To compute a new value of  $z_i$ , one random number is written to the head of the buffer and the indices are updated.

When an event occurs, say the  $(n-1)$ th in Fig. 4, the instant attenuation  $a_T$  is linearly interpolated from two adjacent samples of  $a_{Ti}$ . At the occurrence of the next event, the generating process from Fig. 3 has to advance from time  $t_{n-1}$  to  $t_n$ . If

$$t_n - t_{n-1} < M t_s, \tag{21}$$

An appropriate number of random numbers is updated in the circular buffer to calculate  $a_{T(j-1)}$  and  $a_{Tj}$ . For a longer interval than  $M t_s$  the buffer is simply reinitialized as  $a_T(t_{n-1})$ , and  $a_T(t_n)$  are treated as uncorrelated due to the finite impulse response of the filter.

III. EXAMPLE SIMULATION

Data for the model evaluation at the weak turbulence scenario was obtained from an experimental link with the following parameters:  $\lambda = 1550\text{nm}$ ,  $L = 500\text{m}$ ,  $D = 25\text{mm}$ ,  $R = 125\text{Mbps}$  [17]. The sampling frequency was 10 kHz with a 2 kHz anti-aliasing filter. Fig. 5 shows a 0.5 s interval of  $a_T$ , which also represents the normalized received power.

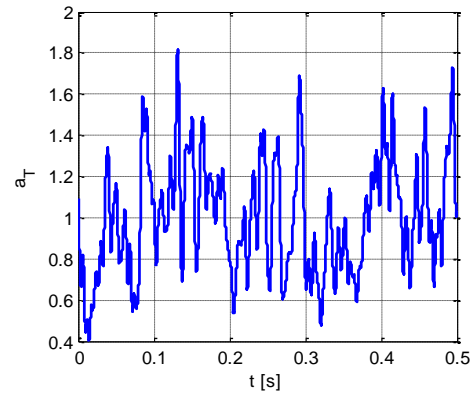


Fig. 5 Normalized received power from experimental link

The power scintillation index  $\sigma_T^2 = 0.12$  was calculated for a 20s interval during cloudy weather (low  $C_n^2$ ).

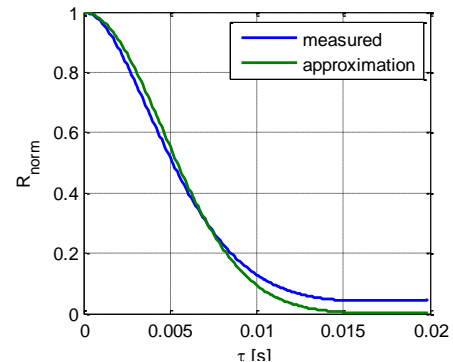


Fig. 6 Normalized autocorrelation function of  $a_T$

Fig. 6 shows the normalized autocorrelation function from which  $\tau_0 = 6.5$  ms was identified. The figure shows that the theoretical function (15) decays quickly in comparison with measured data, i.e. the low-frequency components of the generated signal will be weaker.

The FIR filter was designed using a 64-point FFT with the sampling time  $t_s = \tau_0/5 = 1.3\text{ms}$ . 32 points of the calculated and windowed impulse response were used for filter coefficients.

The procedure used assures the same PSI of the generated  $a_T$ . The time domain properties, which are relevant to communication protocol modeling, are demonstrated in Fig. 7. The channel-good-time represents an interval where the received power is greater than a chosen threshold. Fig. 7 shows the complementary cumulative distribution function of channel-good-times for the chosen threshold  $a_T = 1.5$ .

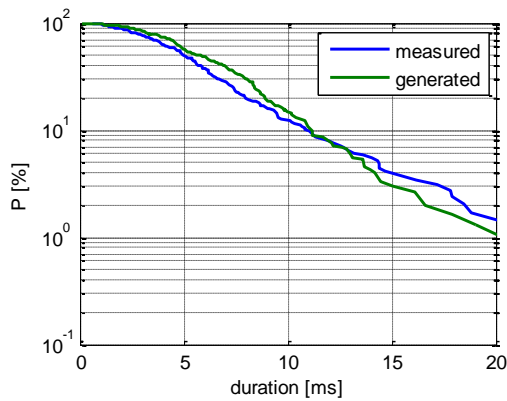


Fig. 7 Complementary cumulative distribution function of channel-good-times for threshold  $a_T = 1.5$

#### IV. CONCLUSION

The paper presents a fully parameterized model for simulating packet transmission on FSO channels by generating random levels of received power. Both statistics and autocorrelation properties of the generated signal agree with data measured on the test link.

The depth of turbulence can be set by specifying PSI directly or by estimating it from  $C_n^2$  and optical terminal parameters using (11)-(14). The “frequency” of turbulence can be specified by channel correlation time  $\tau_0$  directly or by providing the crosswind speed  $v_{\perp}$  in (16).

#### ACKNOWLEDGMENT

This work has been supported by the Czech Science Foundation under grant No. P102/11/1376, by the Czech Ministry of Industry and Trade under grant agreements No.FR-TI4/148 and No. FR-TI2/705, by the Technology Agency of the Czech Republic under grant agreement No. TA02030845, and by and the Project for the development of K217 Department, UD Brno. The research described was performed in laboratories supported by the SIX project, registration number CZ.1.05/ 2.1.00/03.0072, operational programme Research and Development for Innovation.

#### REFERENCES

- [1] H. Henniger, B. Epple, and D. Giggenbach, “Mobile FSO Activities in Europe and Fading Mitigation Approaches,” in *Proc. 17th Int'l. Conf. Radioelektronika*, 2007, pp. 1-6.
- [2] Z. Ghassemlooy, W. Popoola, and S. Rajbhandari, *Optical Wireless Communications System and Channel Modelling with MATLAB*, CRC Press, 2012.
- [3] Z. Kolka, O. Wilfert, and O. Fiser, “Achievable qualitative parameters of optical wireless links,” *J. Optoelect. Adv. Mat.*, vol. 9, no. 8, August 2007, pp. 2419 – 2423.
- [4] I. I. Kim, B. McArthur, and E. Korevaar, “Comparison of laser beam propagation at 785 nm and 1550 nm in fog and haze for optical wireless communications,” *Proc. of SPIE*, vol. 4214, 2001, pp. 26-37.

- [5] F. Nadeem, V. Kvicera, M. S. Awan, E. Leitgeb, S. S. Muhammad, and G. Kandas, “Weather Effects on Hybrid FSO/RF Communication Link,” *IEEE J. Sel. Areas in Comm.*, vol.27, no.9, Dec. 2009, pp. 1687-1697.
- [6] L.C. Andrews, C.Y. Phillips, and J. Hopen, *Laser Beam Scintillation with Applications*, SPIE Press, Bellingham (WA), USA, 2001.
- [7] M. Uysal, J. Li, and M. Yu, “Error Rate Performance Analysis of Coded Free-Space Optical Links over Gamma-Gamma Atmospheric Turbulence Channels,” *IEEE Trans. on Wireless Comm.*, vol. 5, no. 6, 2006, pp. 1229 – 1233.
- [8] V. V. Mai, T. C. Thang, and A. T. Pham, “Performance Analysis of TCP over Free-Space Optical Links with ARQ-SR,” in *Proc. of the 18th European Conference on Networks and Optical Communications (NOC 2013)*, Graz, Austria, 2013, pp. 105-112.
- [9] E.J. Lee and V.W.S. Chan, “Performance of the transport layer protocol for diversity communication over the clear turbulent atmospheric optical channel,” in *Proc. of 2005 IEEE International Conference on Communications*, 2005, pp. 333-339.
- [10] D. K Borah, A. C. Boucouvalas, C. C. Davis, S. Hranilovic, and K. Yiannopoulos, “A review of communication-oriented optical wireless systems,” *EURASIP Journal on Wireless Communications and Networking*, 2012:91 doi:10.1186/1687-1499-2012-91.
- [11] F. Davidson, C.J. Juan, and A.R. Hammons, “Channel fade modeling for free-space optical links,” in *Proc. of Military Communications Conference (MILCOM 2010)*, San Jose, USA, pp. 802-807.
- [12] A. Mostafa and S. Hranilovic, “Channel Measurement and Markov Modeling of an Urban Free-Space Optical Link,” *IEEE/OSA Journal of Optical Communications and Networking*, vol.4, no.10, pp. 836-846.
- [13] A. Jurado-Navas, J.M. Garrido-Balsells, M. Castillo-Vázquez, and A. Puerta-Notario, “A Computationally Efficient Numerical Simulation for Generating Atmospheric Optical Scintillations. Numerical Simulations of Physical and Engineering Processes,” J. Awrejcewicz (Ed.), InTech, 2011, DOI: 10.5772/25139.
- [14] N. Perlot, “Evaluation of the scintillation loss for optical communication systems with direct detection,” *Optical Engineering*, vol. 46, no. 2, 2007, pp. 025003.
- [15] F.S. Vetelino, C. Young, L. Andrews, and J. Rekolons, “Aperture averaging effects on the probability density of irradiance fluctuations in moderate-to-strong turbulence,” *Applied Optics*, April 2007, vol. 46, no. 11, pp. 2099-2108.
- [16] A.V. Oppenheim, R.V. Schaffer, and J.R. Buck, *Discrete-Time Signal Processing (2nd ed.)*, Prentice-Hall, 1999.
- [17] M. Kubicek, H. Henniger, and Z. Kolka, “Bit error distribution measurements in the atmospheric optical fading channel,” *Proc. of SPIE*, vol. 6877, 2008.